Available online at www.sciencedirect.com
ScienceDirect
Nuclear Instruments and Methods in Physics Research A 574 (2007) 28–38
NUCLEAR INSTRUMENTS & METHODS IN PHYSICS RESEARCH Section A
www.elsevier.com/locate/nima

Long term performance and ageing of CsI photocathodes for the ALICE/HMPID detector

H. Hoedlmoser[a,*], A. Braem[a], G. De Cataldo[a,b], M. Davenport[a], A. Di Mauro[a], A. Franco[b], A. Gallas[b], P. Martinengo[a], E. Nappi[b], F. Piuz[a], E. Schyns[a]

[a]*CERN, Switzerland*
[b]*INFN-Sez. di Bari, Bari, Italy*

Received 6 December 2006; received in revised form 11 January 2007; accepted 11 January 2007
Available online 1 February 2007

Abstract

The performance of CsI photocathodes for the ALICE/HMPID detector with regard to long term stability and ageing effects has been investigated and monitored during the production phase and in dedicated ageing tests. During normal storage and test beam operations none of the monitored PCs has showed a decrease in quality within a time-frame of two years. In accelerated ageing tests with ion-bombardment in the detector caused by ionizing particles, pronounced ageing effects could be observed for charge doses $\geqslant 1\,\mathrm{mC/cm^2}$, whereas irradiations with $\leqslant 0.2\,\mathrm{mC/cm^2}$ showed no effect.

PACS: 25.6; 34.8a

Keywords: CsI photocathode; Stability; Ageing; RICH; HMPID; ALICE

1. Introduction

The ALICE High Momentum Particle Identification (HMPID) detector [1,2] is a Ring Imageing Cherenkov (RICH) detector in a proximity focussing layout in which the primary ionizing particle generates Cherenkov light inside a liquid C_6F_{14} radiator. The UV photons are converted into photoelectrons in the 300 nm thin CsI film of the photocathodes (PCs) and the photoelectrons are amplified in an avalanche process inside a Multi-Wire Proportional Chamber (MWPC) operated with CH_4. To obtain position sensitivity for the reconstruction of the Cherenkov rings, the PCs are segmented into pads ($8 \times 8.4\,\mathrm{mm^2}$). Details about the technical design are given in Ref. [2] and the current status of the ALICE HMPID project is described in Ref. [3]. The production of the CsI PCs by means of thin film deposition under vacuum has been described in Ref. [4–6]. The quality of the PCs is measured in beam tests and by means of a VUV-scanner system which is integrated into the production setup and allows a fully automated 2D mapping of the photocurrent from the CsI PC resulting from an illumination with a beam of UV light [7,10,11]. The series production of the 42 PCs required to equip the HMPID detector has been summarized in Ref. [4]. This paper focuses on the long term stability of the CsI PC performance under storage and test beam operation as well as on accelerated ageing tests with avalanche ion bombardment inside the MWPC caused by irradiation with a radioactive β source (^{90}Sr). Previously published [12] results concerning stability during the prototype development phase and during operation at STAR and CERN/SPS are complemented by data obtained from the monitoring of PCs since the start of the series production in 2004. In the dedicated ageing tests two PCs received charge doses in the range from $0.2-7\,\mathrm{mC/cm^2}$. Results of the first series of irradiations were already published in Ref. [13], showing considerable degradation for charge doses $\geqslant 1\,\mathrm{mC/cm^2}$ and a post-irradiation self-ageing effect. In this work results from a

*Corresponding author.
E-mail address: herbert.hoedlmoser@cern.ch (H. Hoedlmoser).

0168-9002/$ - see front matter © 2007 Elsevier B.V. All rights reserved.
doi:10.1016/j.nima.2007.01.101

second set of irradiations using smaller charge doses of $0.2\,mC/cm^2$ are presented, which show no degradation, neither immediately after irradiation, nor during a subsequent period of 250 days of repeated measurements. An analysis of some of the samples which received the highest doses by means of X-ray photoelectron spectroscopy (XPS) and secondary electron microscope (SEM) show an excess of carbon on the irradiated samples hinting at an ageing mechanism involving a deposit of hydrocarbons on the surface of the CsI PC.

2. Stability of PCs during storage and test beam operation

The 42 CsI PCs for the HMPID detector have been produced between May 2004 and May 2006. The work in Ref. [4] describes the production procedure and summarizes the results, emphasizing the importance of a heat conditioning phase subsequent to the coating process in order to achieve the required QE. The enhancement effect is believed to be correlated with the removal of water from the surface of the CsI film, which can explain the shift in the photo-emission threshold towards longer wavelength associated with the enhancement effect [4]. A sizable fraction of PCs ($\approx 20\%$) has shown a delayed enhancement. Some of these PCs have been monitored by means of the VUV-scanner system during several months and all of them have shown a slow enhancement as described in the mentioned publication. In addition to these non-standard cases, some of the regular PCs which have achieved a high level of QE immediately after production were rescanned later on to check their stability during storage under Ar gas and beam test operations:

- *PC*50 was produced in June 2004 and rescanned in October 2005 after 470 days of storage under Ar flow and ≈1 week of test-beam operations. The rescan showed an average photocurrent level which was 3% higher than in the measurement after production.
- *PC*53 was produced in August 2004 and rescanned 390 days later in September 2005, showing an 6% increase of the photocurrent compared to the first scan.

In all repeated scans of PCs, both with regular or delayed enhancement, increases at the percent level were found, never a degradation. Another example for the stable performance of PCs is provided by the measurements of the reference areas in the accelerated ageing tests described in the following section. In these irradiations only small parts of a PC were exposed to ion bombardment and the stability of the surrounding non-irradiated areas has been documented over a period of up to 560 days in repeated measurements, as will be described in Section 3.3.2.

3. Ageing tests with avalanche ions

3.1. Experimental setup and the ionic charge measurement

The irradiation was performed using a new detector based on the HMPID design [2] but of a smaller size. It can be equipped with only one full size PC. For the purpose of our study, the HMPID large radiator vessel was replaced by an array of three collimated ^{90}Sr sources and one small C_6F_{14} radiator of 50 mm diameter, located at a distance of 100 mm from the pad plane as shown in Fig. 1, the rest of the parameters of the detector remained identical.

With this geometry, the Cherenkov photons produced by the beam particles filled a circular fiducial region of 148 mm mean radius. As shown in Fig. 1, the axis of each radioactive source intersected the cathode plane around the mean Cherenkov circle orthogonally (Fig. 1(a)). The source angular locations were chosen in such a way that the irradiated zones did not overlap the same anode wires in order to facilitate the anode and pad current read-out. The collimator distance to the cathode pad plane was chosen so that the region of maximum irradiation density covered an array of 4×4 pads (pad size $8.0 \times 8.4\,mm^2$). This area was in turn overlapped by the Cherenkov fiducial zone allowing to compare the CsI-QE of irradiated spots with the remaining region. Moreover at each spot, 20 pads of the irradiated zones were connected together in order to measure the integrated charge dose given by the cathode current generated during the irradiation. In addition to the measurement of the anodic and cathodic currents, every pad signal was recorded by the FEE (based on the GASSIPLEX analog multiplexed read-out [8]) using the anode signals as a trigger. The spots were irradiated using ^{90}Sr sources of either 2.9 or 29.9 or 260 MBq activity (see Table 1).

At each position, only the 8 anode wires in front of the 4×4 pad array were raised to the working amplification voltage, the rest of the anode plane was kept at 1000 V. This way gas amplification—and consequently also the possibility for ageing effects—was restricted to a strip of $33.6 \times 640\,mm^2$. The currents of the 8 wires (I_{8anode}) and of the 20 pads (I_{20pads}) were recorded using a CAEN-N671A[1] power supply and a Keithley[2] 617 pico-amperemeter, respectively. The values of the HV, currents, pressure of the gas inside the MWPC and temperature were monitored and recorded every second using part of the HMPID Control System [9] based on the industrial SCADA product PVSS[3] adopted at CERN for the LHC experiments. The gas used was CH_4. Before the insertion in the detector, the PC was kept in an encapsulated protective box under dry Ar flow. The insertion was done in a custom made glove box under a controlled Ar atmosphere. The total volume of the detector is 21.5 l, during the irradiation

[1]CAEN SpA, 55049 Viareggio, Italy.
[2]Keithley Instr. Inc. Cleveland, 44139 Ohio, USA.
[3]SCADA system by ETM AG (Eisenstadt, Austria): http://www.etm.at/

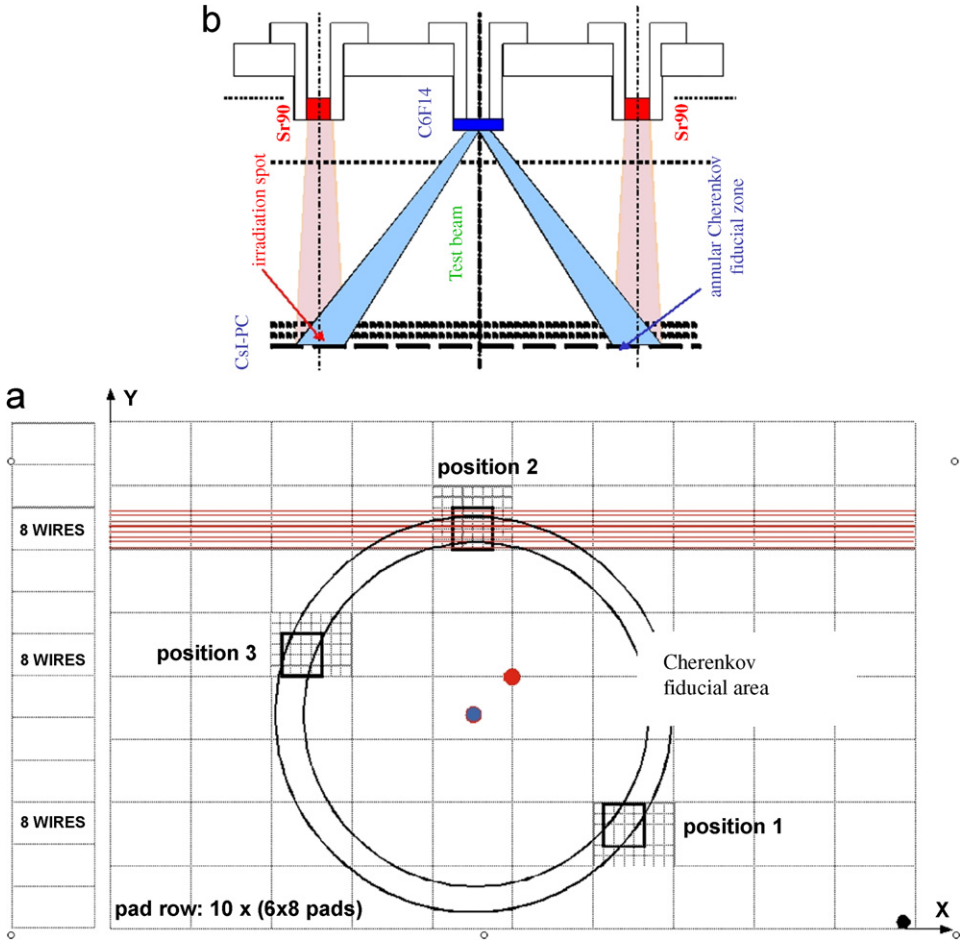

Fig. 1. (a) The locations of the three irradiation spots. The anode wires are horizontal (X-coordinate). The Cherenkov annular zone overlaps the three spots; a fourth spot for irradiation could be obtained by turning the PC 180° inside the chamber. (b) Cross-section of the detector along a plane containing the centers of the radiator and spots 1 and 3. The RICH has a proximity focusing geometry, with an electrode collecting the ionization deposited along the proximity gap. The MWPC has a 2 mm half-gap, 4.2 mm anode pitch. The pad size is $8.0 \times 8.4\,mm^2$, all coated with CsI. The chamber gas is CH_4. Each ^{90}Sr source is embedded in a Plexiglas cylinder and collimated by a 10 mm long hole, 4 mm diameter, closed by a 50 μm thick Mylar foil.

Table 1
List of irradiations on PCs 39 and 58

PC ID	Position no.	Source activity (MBq)	Duration of irrad. (h)	MWPC anode voltage (V)	Accumulated charge (mC/cm^2)	Dose rate (mC/cm^2 (h)	Eq. running time ALICE p–p and Pb–Pb (y)
PC39	Pos. 1	29.9	196.3	2167	6.31	0.032	121
PC39	Pos. 2	260	192.0	1980	6.79	0.035	131
PC39	Pos. 3	260	48.0	1980	1.54	0.032	30
PC39	Pos. 4	29.9	100.9	2050	0.97	0.010	18.7
PC58	Pos. 1	254	18.6	2050	0.193	0.010	3.7
PC58	Pos. 2	29.9	96	2050	1.106	0.012	21.3
PC58	Pos. 3	2.9	292.7	2050	0.196	0.001	3.8

the flow was always $\geqslant 20$ l/h. The purity and composition of the used gases is shown in Table 2. The levels of oxygen and water impurities were always lower than 10 and 5 ppm, respectively, during storage and operation, and the level of hydrocarbons in the methane during operation was $\leqslant 200$ ppm C_2H_6 and $\leqslant 50$ ppm for other C_nH_m. The PC sees highest levels of impurities during transfer to and from the detector in the glove box and after the irradiations when it is transferred to the VUV scanner for the evaluation of the photocurrent as described in Section 3.3.

The proportionality of the amplification regime was checked up to the maximum voltage used of 2167 V. The currents were found perfectly stable up to eight days of continuous irradiation, indicating that no anodic ageing was induced. Besides the mentioned irradiation tests, short runs were taken at lower rates to measure the charge pad profile as shown in Fig. 2. The ionic charge densities, Qint

Table 2
Composition and impurities of the CH_4/Ar gas used to operate/store the MWPC

Gas	CH_4	Ar
Purity (%)	>99.95	>99.998
Impurities		
O_2 (ppm)	<10	<2
H_2O (ppm)	<5	<3
N_2 (ppm)	<200	<10
H_2 (ppm)	<20	<1
C_2H_6 (ppm)	<200	
CO_2 (ppm)	<10	<1
C_nH_m (ppm)	<50	
CH_4 (ppm)		<1

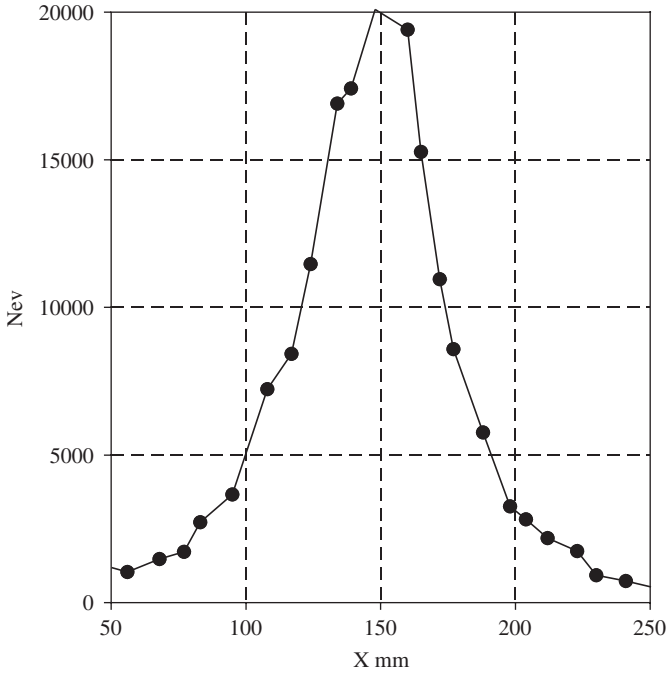

Fig. 2. Ionic charge profiles: along the X-coordinate obtained from the distribution of the charge centroids of the pad clusters.

($A\,cm^{-2}$), could be derived from the integration of the current measured at the 4×5 pads along the anode wires during the irradiations. It was checked that the same densities could be derived from the anodic currents. In total seven irradiations were performed, four on PC39 and three on PC58—see Table 1.

3.2. Expected charge dose in ALICE

The ALICE experiment is characterized by a low event rate, in the range of a few 10^4-10^5 Hz in Pb–Pb and p–p collisions, respectively. However, high multiplicities are expected, reaching for central Pb–Pb collisions 100 particles/m^2 in the HMPID modules located at 5 m from the vertex. The expected charge dose for 10 years operation is estimated to be 0.52 mC/cm^2, shared as 0.45 and 0.07 mC/cm^2 between p–p and Pb–Pb events, respectively [15]. Table 1 lists both the accumulated charges and the equivalent running times in ALICE for the seven irradiations performed in the ageing tests. The charge doses applied in the irradiations of PC39 have been rather high compared to the equivalent running time in ALICE, however these measurements also were some of the first tests of the sensitivity of the VUV scanner, and consequently high doses have been used to induce a clearly measurable effect. Only in the next series of irradiations on PC58 the doses were lowered to a level which is more realistic for the ALICE/HMPID application.

3.3. Photocurrent decrease in aged areas

As described in Refs. [13,7,11] the effect of the irradiation on the PC QE was investigated through a mapping of the photocurrent over the full PC surface including the irradiated areas in the above mentioned VUV-scanner. The irradiated PCs were installed inside the scanner enclosed with a protective box filled with Ar.[4] After installation in the chamber the whole vacuum tank of the VUV scanner (1000 l) has to be purged with Ar until the purity is good enough to open the protective box and start the pumps. In this procedure the oxygen concentration is measured at the output of the chamber, and the PC is opened at a level of <500 ppm. Immediately afterwards the pumps are started and it takes roughly 30 min until the chamber is evacuated to a safe level.

The scanner records the photocurrent I_{CsI} from the PC as well as the reference signal I_{PM} from a photomultiplier (PM) (read from the first dynode without amplification) and the background levels $I_{CsInoise}$ and $I_{PMnoise}$. The reference current on the PM is used to normalize the photocurrent from the PC according to $I_{norm} = (I_{CsI} - I_{CsInoise})/(I_{PM} - I_{PMnoise})$. By comparing I_{norm} of irradiated and non-irradiated areas on the PC the ageing-induced drop in photocurrent could be measured. Fig. 3 shows the normalized photocurrent measured on PC39 clearly exhibiting the effect of the high-dose irradiations on positions 1–4 (compare Table 1).

To quantify the QE drop for a given irradiated position, the average $\langle I_{norm}\rangle_{irrad}$ over the sixteen lowest values of I_{norm} inside the irradiated zone (corresponding to the 16 pads in the center of the irradiation cone) was compared with a reference value $\langle I_{norm}\rangle_{ref}$, which was calculated by taking an average over all the scanned positions outside the irradiated zone. Usually a 280 point scan is performed on the whole PC to provide this reference. The QE drop was expressed as

$$\frac{\Delta QE}{QE} = \frac{\langle I_{norm}\rangle_{ref} - \langle I_{norm}\rangle_{irrad}}{\langle I_{norm}\rangle_{ref}}. \quad (1)$$

[4]The Ar flow was only interrupted for the duration of the transport between glove box or storage and the VUV scanner.

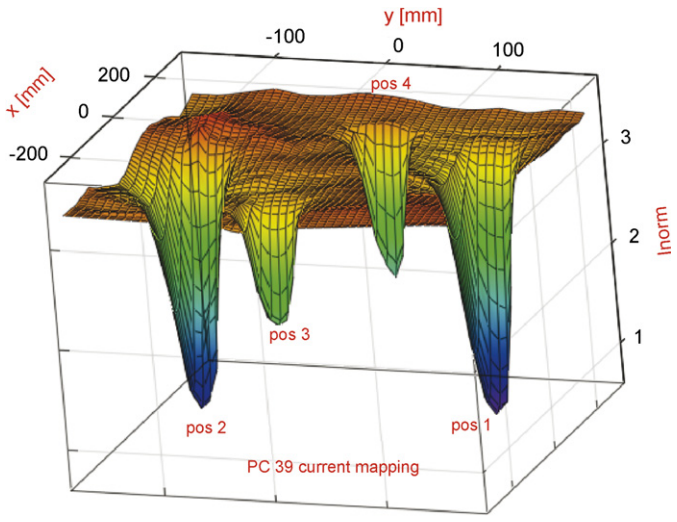

Fig. 3. Mapping of the photocurrent on PC39 several months after the irradiation tests. A clear degradation of the photocurrent in the four irradiated areas is visible.

The photocurrent measurements were performed with a deuterium lamp[5] and UV optics containing CaF_2 windows [7,11]. By means of a removable quartz window in the optical path to cut the UV spectrum of the lamp below 180 nm, the measurements could be performed with two different spectra, which did not influence (compare Ref. [11]) the obtained values of $\Delta QE/QE$—consequently the observed ageing effect seems to be independent of photon wavelength. Values for $\Delta QE/QE$ obtained from scans as in Fig. 3 will be given in Section 3.3.2, which discusses the time development of the measured effect.

3.3.1. Correlation of charge and damage profiles

Fig. 4 shows a contour plot of the photocurrent measured on PC39 after the first three irradiations. It can be seen that the decreased zones are elongated in x direction, which is the direction of the wires inside the detector as indicated in Fig. 1(b). This is due to the fact that the irradiation profile is widened by scattered electrons as can also be seen in the ionic charge profile in Fig. 2. Across the wires in y direction on the other hand the drop in QE is sharp and localized to an area of roughly 3–4 cm which corresponds to the 4 pads or 8 anode wires which were powered during irradiation. Therefore it can be concluded that the QE decrease is actually due to the ion bombardment and not a consequence of the primary irradiation from the radioactive source. In the case of high dose irradiations a comparison of charge profiles such as given in Fig. 2 and the damage profiles obtained from scans like presented in Figs. 4 and 3 was used to derive a correlation between the damage and charge dose. The corresponding dose-effect plots have been published in Ref. [13,11]; however, they are of limited applicability due to the time dependence of the effects, described in the following section (Section 3.3.2). For the sake of completeness, it should also be repeated here that the local degradation of the photosensitivity of PC39 was confirmed in a beam test. In this test multiple Cherenkov events were analyzed which contained the three irradiated positions 1–3 inside the fiducial zone (compare Refs. [13,11]). The photon yield within the Cherenkov ring showed a comparable degradation.

3.3.2. Long term behavior of QE decrease

The actual test sequence in the irradiations of PC39, as summarized in Table 1, was at first an irradiation of position 2, followed by a scan, which showed a $\Delta QE/QE$ of 0.4. It was also attempted to heat the PC up to 60 °C for 20 h under vacuum, which did not change the QE drop in the irradiated zone. Afterwards the positions 1 and 3 were irradiated, followed by an analysis of the PC response in a beam test [13,11], and further evaluations in the VUV-scanner. When the PC was scanned the second time, it turned out that the QE drop measured in position 2 had increased to 0.7, although this position had not seen any more radiation in the second series of irradiations in positions 1 and 3. The first two scans of position 2 are given in Fig. 5.

Following these observations, the PC was rescanned several times and irradiated in a fourth position. The photocurrent was monitored in eight scans covering a total duration of 560 days. In-between scans the PC was stored under Ar flow of at least 10 l/h. At all stages (storage, test-beam operations, transfers) the PC was kept either under Ar or under methane in the beam test. The QE decrease as a function of time recorded for each of the four irradiated positions is shown in Fig. 6. A possible explanation of this effect is a reaction of the irradiated areas with contaminations in the gas. This hypothesis is strengthened by the observation, that the effect is not progressing when the PC is kept under vacuum. In one test PC39 was kept under vacuum for 10 days and no further increase of the QE drop could be observed. Due to time constraints imposed by the series production of PCs [4] the VUV-scanner was not available to keep an irradiated PC under vacuum for an extended period (months) for a final verification of this hypothesis. Furthermore, Fig. 6 shows the change of the average reference current $\langle I_{\mathrm{norm}}\rangle_{\mathrm{ref}}$ outside the irradiated zones in time (empty squares). The change in the reference level was calculated with respect to the first measurement following the first irradiation. It follows that in the observed time-frame of 560 days the average current level outside the irradiated zones did not change by more than 5% which proves both the stability of the PC and the effectiveness of the handling procedures during installations and transfers.

3.3.3. Dose threshold for ageing effect

Following the irradiations with high accumulated charges on PC39 a new series of irradiations was performed on PC58. Position 2 was irradiated with 1 mC/cm^2 to

[5]Hamamatsu L7292 with a MgF_2 window (http://www.sales.hamamatsu.com/).

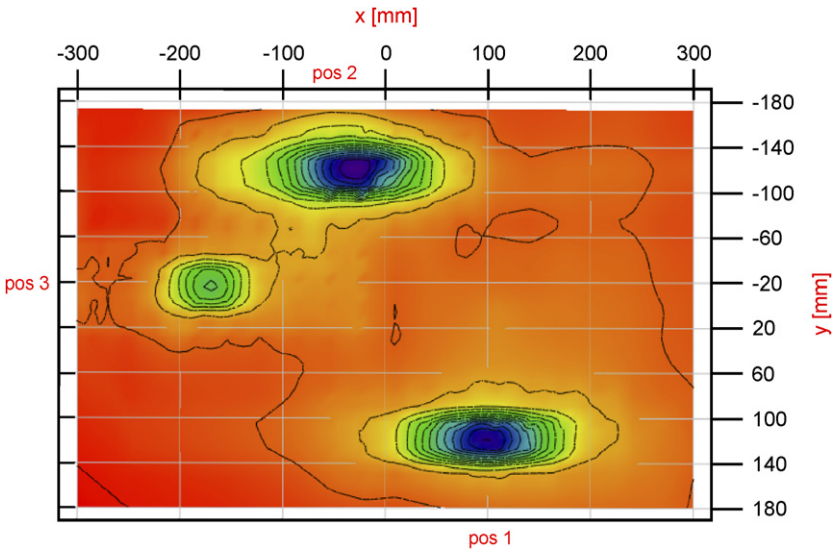

Fig. 4. Contour plot of the photocurrent measured on PC39 after the first three irradiations. The aim of the plot is to show the elongated shape of the damaged zones along the direction of the anode wires (x) and the sharp narrow profile across the wires (y) due to the fact that only 8 wires have been powered.

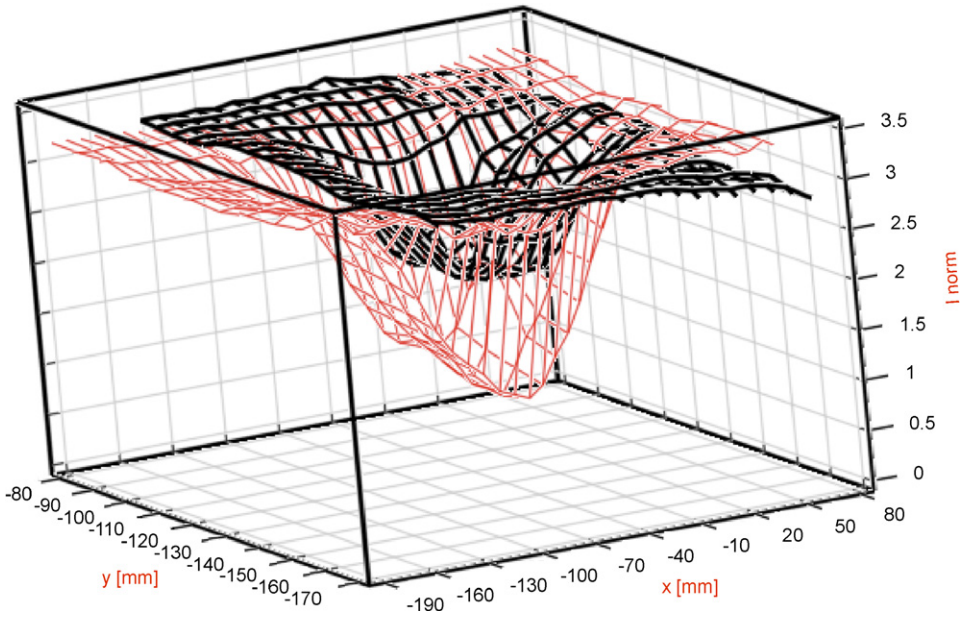

Fig. 5. Photocurrent scan on position 2 on PC39 immediately after irradiation (thick wireframe) and 110 days after irradiation (thin wireframe). In the second scan the QE degradation was more severe (70%) than in the first (40%).

reproduce the results of position 4 on PC39. Positions 1 and 3 on PC58 received 0.2 mC/cm^2. See Table. 1. The QE drop measured for the irradiation with 1 mC/cm^2 was initially approximately 25%, which is more than what was to be expected from the comparable position 4 on PC39. The QE drop showed a similar time development as the ones measured on PC39, increasing to 55% within 250 days after irradiation. The two positions irradiated with 0.2 mC/cm^2, however, did not show any degradation. Fig. 7 shows a scan of PC58 taken 250 days after the irradiations. Only the 55% QE drop on the position irradiated with 1 mC/cm^2 is visible, the other two positions show no measurable degradation.

3.4. Surface analysis of irradiated areas

Samples from the irradiated positions on PC39 were visually inspected and analyzed both in a secondary electron microscope (SEM) and in a setup for X-ray photoelectron spectroscopy (XPS).

3.4.1. Sample preparation

The 18×18 mm^2 samples were cut out from the irradiated areas of the large area PC in a procedure reducing any contamination of the CsI surface to a minimum and avoiding contact with air: at first the connectors were removed from the backside of the still

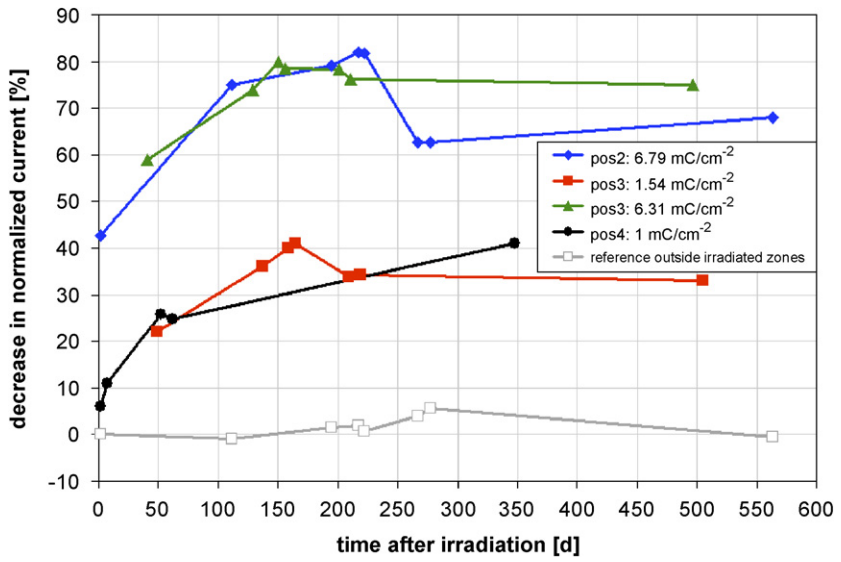

Fig. 6. Development of the QE drop in the four irradiated positions on PC39 in time after irradiation. The degradation of the QE in the irradiated zones is progressing in time while the reference measured in the non-irradiated areas is stable (empty squares). In-between scans the PC was stored under Ar flow of at least 10 l/h.

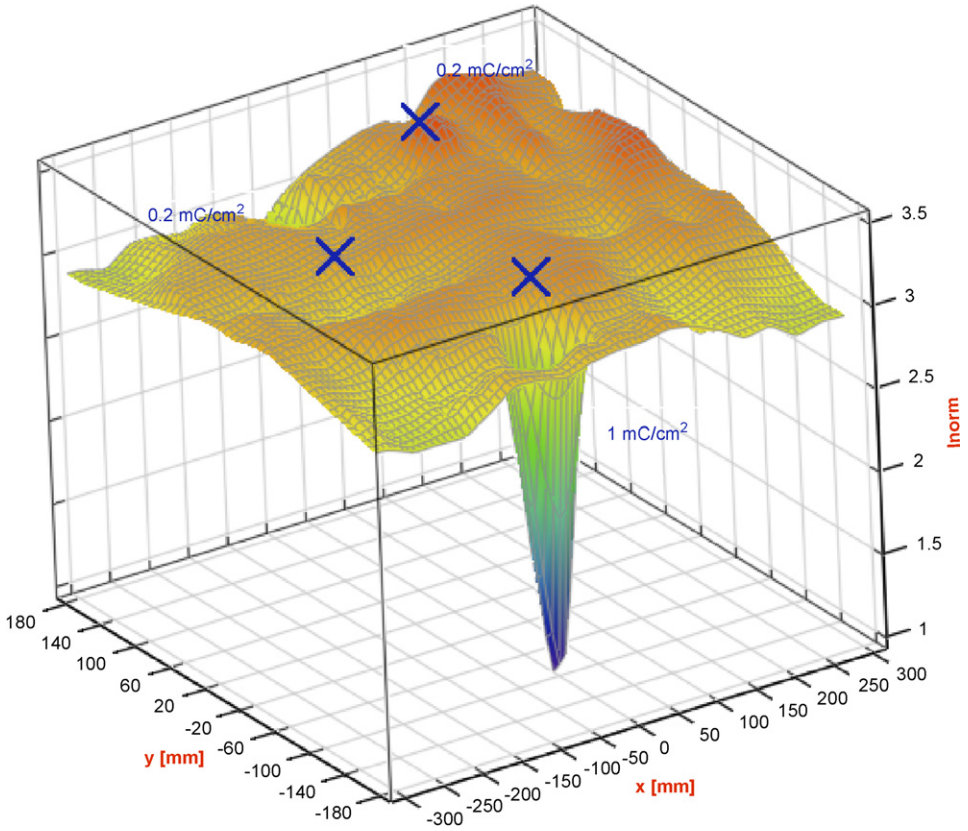

Fig. 7. Scan of PC58 250 days after irradiations. The irradiated positions are marked with blue crosses above the plot. The positions irradiated with 0.2 mC/cm^2 exhibit no measurable QE drop.

enclosed PC. The PCB substrate was subsequently pre-cut with a machining tool up to a few tenths of a mm below the front surface of the PC. Afterwards the PC was transferred into a glove box and opened under Ar atmosphere, where the final cutting through the front surface was performed with a stainless steel scalpel. The samples were then enclosed under Ar either in a sample-holder for the SEM or sealed in steel pipes for transport to the XPS. Samples were always prepared in pairs, one irradiated sample and one reference sample from a non-irradiated area of the PC.

3.4.2. Visual observations

In the glove box the samples could be visually examined. Of the four irradiated positions on PC39 only position 2, which had received the highest charge dose, showed a visual sign of the irradiation in the form of purplish stripes positioned exactly under the anode wires of the chamber—see Fig. 8. Position 1, which has received a similar charge dose, showed no visible marks.

3.4.3. SEM analysis

Samples from positions 1 and 2 together with reference samples were transferred to the SEM without exposure to ambient air. The electron microscope pictures showed the expected CsI grain structure on all samples—see Fig. 9 right side. On the sample from the irradiated position 2, which exhibited the purplish stripes in the visual examination (Fig. 8), dark spots with a crack at the center were found in the locations of the stripes, as is shown in Fig. 9. The left side shows the dark spots in low magnification, whereas the right picture shows the grain structure and the dark regions with the cracks in higher magnification. Apart from the black spots on the sample from position 2 no differences could be found between the reference samples and the irradiated samples. The sample from position 1 was indistinguishable from the reference samples. This might be due to a rather bad surface sensitivity of the SEM investigation. Depending on beam energy the electrons penetrate the film up to a thickness of a micron. The secondary electrons, which are used to create a picture originate from a fraction of this thickness, e.g. up to 100 nm corresponding to up to 200–300 mono-layers (ML) CsI, therefore any signal e.g. from a deposit of a few layers of carbon on top, as suggested by the results of the XPS analysis (Section 3.4.4) might be difficult to see in the SEM pictures. The dark spots visible on the samples of position 2 could be interpreted as the thickest areas of a carbon deposit on the CsI. Due to the lower secondary electron yield of carbon, it would appear dark in a SEM picture.

3.4.4. XPS analysis

To obtain chemical information about the surface composition of the samples, they were also analyzed in a XPS setup, which provides a much better surface sensitivity. Taking into account the inelastic mean free paths of photoelectrons emitted from Cs, I, C, and O in CsI, the 45° analysis angle of the setup and some correction for elastic scattering, the investigation depth of the system can be assumed to be less than 20 nm. The ability of the method to identify the chemical elements on a surface allows to look for signs of some particular ageing mechanisms, e.g. the presence of carbon could indicate a deposit produced by the CH_4 ions, probably due to a polymerization reaction [14], and an excess of Cs (and O) would support the "Cesiation" hypothesis. In this hypothesis the CsI molecules are dissociated in the charge neutralization of the avalanche ions, which results in the formation and evaporation of I_2 at the surface and consequently an excess of Cs at the surface, which in turn might oxidize in contact with oxygen contaminations in the chamber gas.

The drawback of the XPS method is the necessity to expose the samples to air for about 2 min while they are being mounted on a sample holder. It is known that any exposure to air causes adsorption of water, molecular oxygen, and hydro-carbons, which increases the signal of O and C in the following XPS analysis. In a dedicated test, a non-irradiated reference sample from PC39 was transferred from the glove box to the XPS system with the minimum amount of exposure possible. The analysis of several positions showed an average concentration of 27.3% C and 1.5% O. Afterwards the sample was exposed to air for

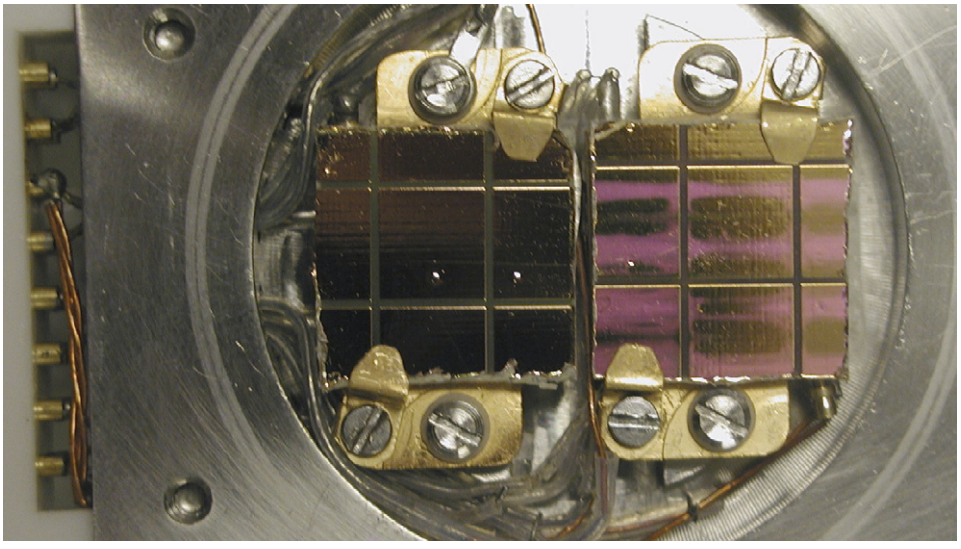

Fig. 8. Sample from position 2 (right) and from a non-irradiated reference area (left) mounted on a sample-holder for transport to the SEM. The irradiated sample shows stains at the positions below the anode wires.

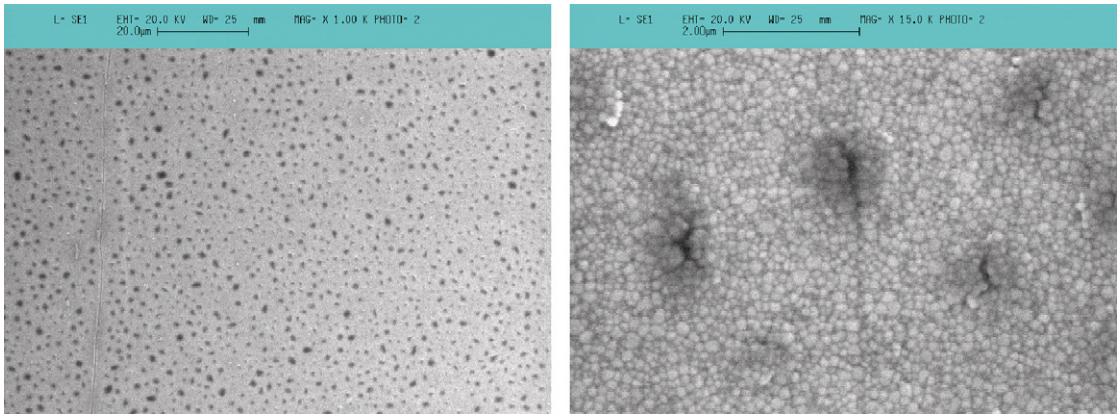

Fig. 9. SEM pictures in two different magnifications from the irradiated position 2. The purplish stains from Fig. 8 correlate with the presence of black spots.

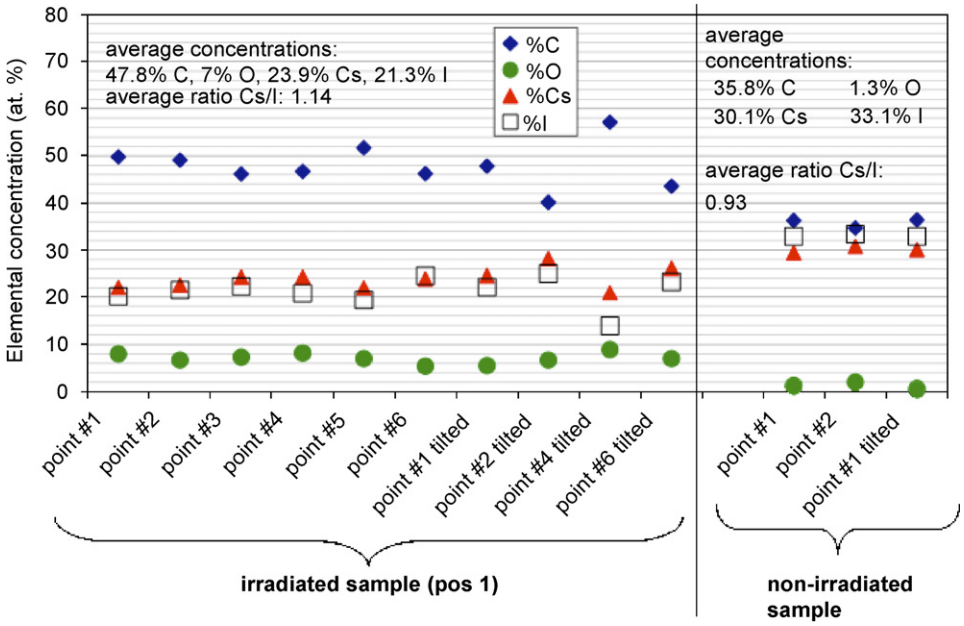

Fig. 10. XPS analysis of an irradiated sample from position 1 and a non-irradiated reference sample. The investigated positions on the irradiated sample show an average concentration of 47.8% C and 7% O, whereas the concentrations on the reference sample are 35.8% C and 1.3% O.

15 min and the analysis was repeated. The concentrations of C and O had risen to 46% and 4.7%, respectively. As a consequence it was only possible to compare irradiated and non-irradiated samples with a very similar exposure history. In total three sets of samples, composed of one irradiated and one non-irradiated sample each, were analyzed. The irradiated samples were taken from positions 1 and 2, which had received the highest doses—see 1. Fig. 10 shows the result of the XPS measurements on a sample from the irradiated position 1 and a reference sample. The average concentrations of C and O on the irradiated sample are significantly higher than on the reference sample. The elevated C concentration indicates a deposit of hydrocarbons, possibly polymers. It could also be argued that the concentration ratio Cs/I is systematically higher on the irradiated sample; however, the effect is very small. Still from these results the "Cesiation" hypothesis cannot be ruled out completely.

The results of the XPS analysis can be summarized as follows:

- All the irradiated samples of positions 1 and 2 showed a higher concentration of C and O in direct comparison with a reference sample with the same history of exposure.
- The highest concentrations of C were measured on the sample of position 2 exhibiting the stains.
- The oxygen peak in the XPS spectra was too small to detect a possible chemical shift, therefore no conclusions about differences in binding states (e.g. O_2, H_2O, CsO_2) can be made.

Clearly these results still leave a lot of room for speculation on the ageing mechanism. A system to transport irradiated samples to the XPS setup without exposure to air would be required to obtain clearer results.

4. Summary and discussion

4.1. Summary

In the following the most important experimental results are summarized briefly:

- Since the start of the series production of CsI PCs in May 2004 all the monitored PCs have shown a stable (in some cases slightly increasing) performance during normal storage or after test beam operations.
- Two standard PCs have been irradiated inside an operative MWPC with a ^{90}Sr source to provoke ageing by avalanche ions. Several positions have been irradiated with accumulated charges up to $7\,mC/cm^2$.
- All positions receiving an accumulated charge dose of $\geqslant 1\,mC/cm^2$ have shown a decrease in photocurrent, which was progressing in time after the irradiation was finished—possibly due to an interaction of the irradiated areas with contaminations in the gas during storage (Ar) or operation (CH_4).
- Heating the irradiated PC to 60 °C during 20 h did not lead to any recovery of the photocurrent in the irradiated areas—compare Ref. [11].
- The decrease of the photocurrent was measured with two different UV source spectra (with and without quartz window) leading to the same result. This indicates no strong wavelength dependency of the ageing effect—see Ref. [11].
- Two positions irradiated with an accumulated charge dose of $0.2\,mC/cm^2$ have not exhibited any measurable decrease in photocurrent, neither immediately after irradiation, nor up to 250 days after irradiation.
- The surface analysis of samples from the highly irradiated positions ($7\,mC/cm^2$) by means of XPS and SEM have shown higher concentrations of C and O in the irradiated regions. A small excess of Cs cannot be ruled out from the results.

4.2. Discussion of the results

Although the ageing of CsI photocathodes is a known phenomenon, the underlying physical and chemical mechanisms are still not fully understood. Ageing is discussed for example in Ref. [14] where several mechanisms are summarized. One possible explanation for the presence of carbon in the irradiated sites would be a polymerization reaction as described in Ref. [14]: polymers can form during the avalanche process in a MWPC operated with CH_4 and cause deposits on the electrodes. However, such polymers would also cause wire-ageing, which was not observed as mentioned above. Furthermore, polymers created in the avalanche would move very slowly due to their size and any ageing effect due to a deposit created by adsorption of polymers from the avalanche should consequently depend on the gas flow in the chamber. This could be checked with a series of tests with different gas-flows. Maybe the polymerization reaction rather happens at the surface when the arriving CH_4 ions are neutralized in a CVD[6]-like process.

The observation of a threshold for the ageing effects between charge doses of 0.2 and $1\,mC/cm^2$ could be the consequence of the film growth process. Film growth can usually be described by an adsorption–desorption equilibrium of the arriving molecules on the surface followed by the formation and growth of islands through surface diffusion and capture of new molecules. The diffusion processes as well as adsorption and desorption depend on the binding forces between the substrate and the adsorbed molecules which can change drastically, e.g. as soon as the substrate is covered with a full mono-layer (ML) of the film. This could lead to drastical change in the rate of growth. Furthermore, it should be pointed out here, that the film growth rate usually does not depend linearly on the rate of arriving molecules. E.g. at the beginning of the film growth in the adsorption–desorption equilibrium the number of molecules present at the surface is a linear function of the rate of arriving particles, but already the rate of dimer formation (aggregates of two molecules) depends squarely on the rate of arriving particles. Only if the diffusion and desorption processes can be neglected completely, e.g. in the case of adsorption of polymers which stick very well to the electrodes, the growth rate depends linearly on the rate of the arriving particles. Consequently in any other process the film growth rate can depend strongly on the rate of arriving particles, i.e. on the rate of arriving positive ions in the case of the accelerated ageing test, which in turn is a function of the irradiation rate. This could have a high impact on the validity of an accelerated ageing test per se, which usually assumes a linear dependence between rate and ageing effect to scale the ageing effect to the situation in the real experiment, where the irradiation rates are much lower. In the tests presented above, all the charge dose rates were within one order of magnitude (except for one low charge dose irradiation). To clarify the influence of the dose rate on the ageing effect, the rate should be varied in a much wider range in future tests.

The observed self-ageing after irradiations with high accumulated charge doses, could be explained by a reaction of the irradiated areas with contaminations in the chamber gas or storage gas, as mentioned above. E.g. within the "Cesiation" hypothesis, the ion-bombardment would lead to a higher concentration of Cs on the surface, which would oxidize in the presence of O_2 contaminations in the chamber gas or storage gas. Even a few parts per million (ppm) of O_2 would create a

[6]Chemical vapor deposition.

sufficient O_2 impingement[7] at the surface to result in the oxidation of the free Cs, which could deteriorate the QE further. This hypothesis of a reaction with a contamination in the gas is supported by the observation that the self-ageing seems to stop when the PC is kept under vacuum, which should, however, be tested further by storing an irradiated PC under vacuum for a longer period of time.

5. Conclusion

Clearly the question of the exact ageing mechanism is still open to discussion and many additional tests are required to understand the underlying processes. However, from the results on long term stability and ageing obtained with tests of the ALICE/HMPID PCs, the recently completed HMPID modules are expected to perform particle identification as required in or even exceeding the design specifications for the detector. Especially during the first four years of operation inside the ALICE experiment no ageing effects are expected due to the bombardment with avalanche ions.

Acknowledgments

The operation of the VUV scanner and the production of the PCs relies on the competent support provided by the technical staff at CERN. We would like to thank M. van Stenis, X. Pons, J.B. van Beelen, P. Ijzermans, C. David, M. Malabaila, B. Cantin and D. Fraissard. For the preparation of samples from the irradiated PCs we want to thank J.B. van Beelen. For the XPS and SEM measurements we would like to thank A. Reginelli, M. Taborelli, A. Gerardin and G.A. Izquierdo.

References

[1] ALICE Collaboration, J. Phys. G 30 (2004) 1517.
[2] ALICE Collaboration, ALICE HMPID Technical Design Report, CERN/LHCC 98/19.
[3] A. Gallas, et al., Nucl. Instr. and Meth. A 553 (2005) 345.
[4] H. Hoedlmoser, et al., Nucl. Instr. and Meth. A 566 (2006) 338.
[5] E. Schyns, Nucl. Instr. and Meth. A 494 (2002) 441.
[6] A. Braem, et al., Nucl. Instr. and Meth. A 502 (2003) 205.
[7] H. Hoedlmoser, et al., Nucl. Instr. and Meth. A 566 (2006) 351.
[8] J.C. Santiard, et al., in: Proceedings of the Sixth Workshop on Electronics for the LHC, Snowmass, September 1999, p. 431.
[9] G. De Cataldo, et al., The Detector Control System for the HMPID in the Alice Experiment at LHC, in: 10th ICALEPCS International Conference on Accelerator and Large Experimental Physics Control Systems, Geneva, 10–14 October 2005, PO1.017-1 (2005), ⟨http://elise.epfl.ch/pdf/P1_017.eps⟩.
[10] H. Hoedlmoser, et al., Nucl. Instr. and Meth. A 553 (2005) 140.
[11] H. Hoedlmoser, CERN-THESIS-2006-004, ⟨http://doc.cern.ch/archive/electronic/cern/preprints/thesis/thesis-2006-004.eps⟩.
[12] A. Braem, et al., Nucl. Instr. and Meth. A 515 (2003) 307.
[13] A. Braem, et al., Nucl. Instr. and Meth. A 553 (2005) 187.
[14] J. Vavra, Nucl. Instr. and Meth. A 515 (2003) 1.
[15] A. Morsch, et al., ALICE-INT-2002-28, Geneva, CERN.

[7] One ppm O_2 corresponds to a partial pressure of 10^{-3} mbar. At such a pressure the impingement rate of O_2 at a surface is 2.7×10^{17} molecules $cm^{-2}\,s^{-1}$ compared to a surface density of 4.8×10^{14} molecules cm^{-2} at the CsI surface.